Macromolecules
ARTICLE

Macromolecules **2009**, *42*, 8513–8520 **8513**
DOI: 10.1021/ma9013687

Self-Consistent Field Theory of Gelation in Triblock Copolymer Solutions

Rafael E. Bras and Kenneth R. Shull*

Department of Materials Science and Engineering, Northwestern University, Evanston, Illinois 60208

Received July 6, 2009; Revised Manuscript Received September 9, 2009

ABSTRACT: Self-consistent field theory is applied to study the ordering behavior of triblock copolymer solutions. A unit cell approximation is used that provides information about individual micelles but does not provide information about the 3-dimensional packing of the micellar aggregates. Information obtained from this approach includes the preferred micellar geometry (spheres, cylinders, or lamellar), the aggregation number, bridging fraction, osmotic pressure, and form factor for a scattering experiment. A variety of general conclusions are obtained with regard to the relationships between these quantities and the polymer concentration, end block solvent quality, and relative molecular weights of the different copolymer blocks.

Introduction

Since the first observation of the self-assembly of triblock copolymers, the scientific community has recognized the importance of this class of polymer. The study of multiblock polymer systems has led to a wide variety of applications in everything from car bumpers to new nanolithography techniques.[1−3] Interest in gels formed from triblock copolymers has also increased with the recognition that soft polymeric materials can play an important role as matrix materials in the fields of biomaterials and regenerative medicine. The key feature of triblock copolymer gels that makes them so interesting is their ability to assemble and form elastic solids from viscous liquids in a controlled manner.[4] These materials can be viewed as a subset of "telechelic" polymers with associating end groups,[5] but with end groups having a finite volume that determines the structure of the gel itself.

This paper focuses on applying self-consistent field theory (SCFT) to model the behavior of symmetric ABA acrylic triblock copolymers in a selective solvent. The calculations are closely coupled to a model acrylic system that has been studied extensively in recent years.[4,6,7] These materials undergo a rapid, thermally reversible transition from a liquid to an elastic solid in midblock selective solvents. This transition is driven by the aggregation of polymer end blocks as the solvent−end block interaction parameter increases as the temperature decreases from ∼80 °C to room temperature. End block aggregates are bridged by solvated midblocks, resulting in the formation of a physically cross-linked network. Modeling this process with SCFT provides insight into the details of the experimentally observed gelation phenomenon, which is controlled by a combination of thermodynamic and kinetic factors. For example, coupling between solvent composition of the micelle core and the local glass transition temperature determines the temperature dependence of the relaxation times for the polymer gel.[8] In addition, the distribution of solvent within the gel will affect the temperature dependence of the scattering function. An incorrect or incomplete understanding of these effects can cause experimental results to be misinterpreted.

Self-consistent field theory is a powerful method for modeling the equilibrium behavior of polymer melts and concentrated polymer solutions. The basis of SCFT was developed by Edwards in 1965.[9] Since then, SCFT has been used to describe many features of polymer systems, including the density profiles of polymer brushes,[10,11] the complex phase behavior of block copolymer melts,[12−20] and the dilute solution behavior of micellar block copolymers.[21,22] Modern computational capabilities have extended the application of SCFT by allowing increasingly complex problems to be addressed.[23−28]

In many cases it is appropriate to reduce the full 3-dimensional SCFT simulation to one dimension, using the appropriate symmetry of the system of interest. This practice is known as the unit cell approximation.[29−32] When collapsed to one dimension, the modified diffusion equation derived by Edwards in 1965 is[9]

$$\frac{\partial q(r,n)}{\partial n} = \frac{a^2}{6}\left\{\frac{\partial^2 q(r,n)}{\partial r^2} + \frac{C}{r}\frac{\partial q(r,n)}{\partial r}\right\} - w(r,n)q(r,n) \qquad (1)$$

where C is dependent on system symmetry; $C = 0$ for planar symmetry, $C = 1$ for cylindrical symmetry, and $C = 2$ for spherical symmetry. The distribution function, $q(r,n)$, is related to the probability that polymer a segment, n, is located at a particular position, r, in space. The mean field, $w(r,n)$, is a function of both the local chain composition, dependent on n, and the composition of the surrounding environment. The variable, a, is the polymer statistical segment length.

Detailed descriptions of the use of SCFT techniques for the determination of phase transformations and structural features of block copolymers have been well documented in the references given above. In order to clearly define our own terminology and clarify our use of the unit cell approximation, we briefly summarize our own implementation in the following section. Specific results are then presented for a system that has been well-characterized experimentally.

Theoretical Formulation

The specific self-consistent field theory formulation used in this study is a modified version of the formulation used by Nunalee and Shull for use in polymer melt systems.[20] The starting point for this theoretical formulation is the Flory approximation of the free energy per unit volume, f_{gel}, of a polymer gel:

$$\frac{f_{gel}}{k_b T} = \frac{1}{V_t}\int_V \left\{\Phi_s \mu_s + \Phi_p \frac{\mu_p}{N_p} - \Delta w\right\} - f_{solution} \qquad (2)$$

*Corresponding author. E-mail: k-shull@northwestern.edu.

Published on Web 10/02/2009

where T is the absolute temperature temperature, V_t is the reference volume (defined as the solvent molecular volume), N_p is the length of the polymer (polymer molecular volume normalized by the solvent molecular volume), and Φ are the volume fractions as a function of radial distance from the aggregate center of either copolymer (p) or solvent (s). The terms μ_s and μ_p represent the chemical potentials of the solvent and polymer, while the term Δw enforces the compressibility constraint. The terms ϕ_s, ϕ_p, and Δw are spatially dependent. Additionally, all component degrees of polymerization are normalized by the reference volume so that $N = 1$ for the solvent. The free energy of the gel is normalized using the free energy of a homogeneous solution of polymer, f_{solution}, as a reference. In the reference case $\Delta w = 0$. The chemical potentials for this homogeneous reference case are given by the following expression:[29]

$$\frac{\mu_k}{k_B T} = \ln \phi_k + 1 - N_k \sum_k \frac{\phi_k}{N_k} + \frac{1}{k_b T} \sum_{j=1}^{N_k} w_p(j) \tag{3}$$

The subscript k refers to a particular component, either polymer ($k = p$) or solvent ($k = s$). The first three terms of this expression represent the entropy of component k, while the last term represents the contributions due to thermodynamic interactions between different chemical species:

$$\frac{w_p(j)}{k_b T} = \frac{1}{2} \sum_{m \neq n} \{\phi_m - g_m(j)\} \chi_{mn} \{g_n(j) - \phi_n\} \tag{4}$$

The subscripts m and n refer to the actual chemical species: solvent (s), copolymer end block (a), and copolymer midblock (b). Thus, χ_{mn} represent the various Flory−Huggins interaction parameters. This treatment assumes regular solution behavior, where these interaction parameters are independent of polymer composition. The functions $g_m(j)$ describe the average composition of segment j in component k, where j is an index for each polymer segment going from $j = 1$ at one end of a polymer chain to N_k. The use of this function enables the examination of copolymers with general architectures including multiblock copolymers and gradient copolymers.[33,34]

The incompressibility of the system is enforced by $\Delta w(i)$ according to

$$\frac{\Delta w(i)}{k_b T} = \zeta \{\sum_k \phi_k(i) - 1\} \tag{5}$$

where ζ is inversely proportional to the bulk compressibility. The incompressibility parameter, ζ, is chosen to be large enough so that the results obtained are indistinguishable from the fully incompressible limit where ζ is infinity.

To proceed further, it is necessary to find expressions for the spatially dependent volume fraction in eqs 2−5. This is accomplished by self-consistently solving for the volume fractions of the various components as a function of the system size, which in our case is determined by the location of a reflecting boundary condition. The system size that gives the lowest free energy corresponds to the equilibrium system. During calculations for the volume fractions of the individual components, the overall volume fraction of polymer, Φ_p, is fixed at a desired value. This is achieved by adjusting the solvent chemical potential (μ_s) and polymer chemical potentials (μ_p). There are multiple values for μ_s and μ_p that satisfy these constraints. However, the difference between μ_s and μ_p/N_p for the possible solutions is constant, so that these chemical potentials are uniquely defined from the additional requirement that $\int_v \Delta w = 0$.

Table 1. Number of Segments per End Block and Midblock for the Symmetric ABA Triblock Copolymers Used in SCFT Calculations

polymer	A block length	B block length
long-midblock	231	1225
short-midblock	212	328

One of the results obtained from SCFT calculations is the bridging fraction. The bridging fraction, f_b, is defined as

$$f_b = \frac{\phi_{\text{bridges}}}{\Phi_p} = 1 - \frac{\phi_{\text{loops}}}{\Phi_p} \tag{6}$$

where ϕ_{bridges} is the volume fraction of triblock copolymers whose end blocks are in separate end block aggregates and Φ_p is the total volume fraction of triblock chains. The alternative configuration, quantified by ϕ_{loops}, locates both end blocks in the same aggregate, causing the polymer midblock to form a loop. Calculation of the bridging fraction is achieved by adding an additional step to the recursive SCFT algorithm, which determines the volume fraction of copolymers with only one end block in the same domain.[13,14]

The input parameters used were chosen to correspond to a system for which there is extensive experimental data.[4,6−8] Specific values for the ABA triblocks modeled in this paper are summarized in Table 1. These two polymers have similar end block (A block) lengths, but different midblock (B block) lengths, and are referred to as the "long-midblock" and "short-midblock" polymers throughout this paper.

The temperature-dependent properties of polymer solutions were captured by specifying a temperature dependence for the three χ parameters: χ_{ab}, χ_{as}, and χ_{bs}. We again use values corresponding to the experimental system, where A is poly(methyl methacrylate) (PMMA), B is poly(*n*-butyl acrylate) (PnBA), and the solvent (S) is butanol. For χ_{bs} we use the following temperature dependence:

$$\chi_{bs} = \frac{1}{2} - \frac{A}{2}\left(1 - \frac{\Theta}{T}\right) \tag{7}$$

where T is the absolute temperature, $A = 0.25$, and the theta temperature (Θ) is 303 K. This gives χ_{bs} ranging from 0.50 to 0.41 as the sample is heated from 30 to 95 °C. Values for χ_{as} correspond to published data for PMMA in butanol:[35]

$$\chi_{as} = 4.59 - 0.0115T \tag{8}$$

and range from 1.11 at 30 °C to 0.50 at 83 °C. Distances are normalized by the copolymer radius of gyration, R_g:

$$R_g = a\sqrt{\frac{N_p}{6}} \tag{9}$$

where a the statistical segment length, which is assumed to be equal for the A and B repeat units.

Results and Discussion

SCFT results were obtained using the methods described in the previous section for both the long-midblock and short-midblock architectures. Calculations were carried out for overall polymer volume fractions of 0.10, 0.15, and 0.20. Values for the χ parameters used in the calculations correspond to temperatures ranging from 30 to 80 °C (T from 303 to 353 K in eqs 7 and 8). In the unit cell approximation that we have employed, spherical symmetry is assumed with r representing the radial distance from the center of a core of the A component of the block copolymer.

The micelle size is specified by a surface of mirror symmetry at $r = R$. In this treatment all information about the ordering of the micelles is lost. However, this is not an important limitation for the problems of interest to us because we are interested in properties of the gel that do not depend on the crystalline order of the micelles. Also, by comparison to published 3-dimensional SCFT results for block copolymer melts,[14] we have verified that the unit cell approximation accurately captures the location of order/disorder and order/order transitions between disordered, spherical, and cylindrical domain morphologies. In the following subsections we describe results pertaining to the fundamental structure of the polymer gel, the fraction of bridging midblock chains, the osmotic properties of the gel, and the X-ray scattering structure factor.

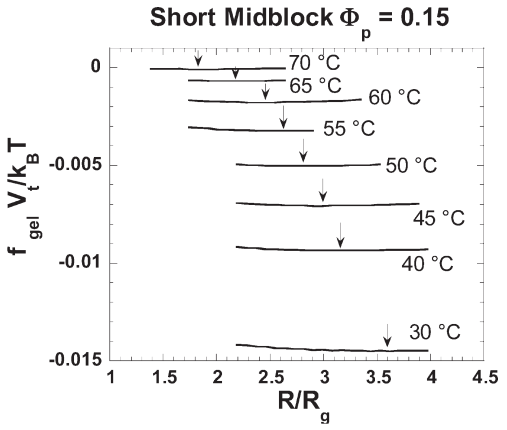

Figure 1. Free energy as a function of micelle size for the short-midblock polymer for $\Phi_p = 0.15$ and $T = 50$ °C. The arrows correspond to $R = R_{eq}$.

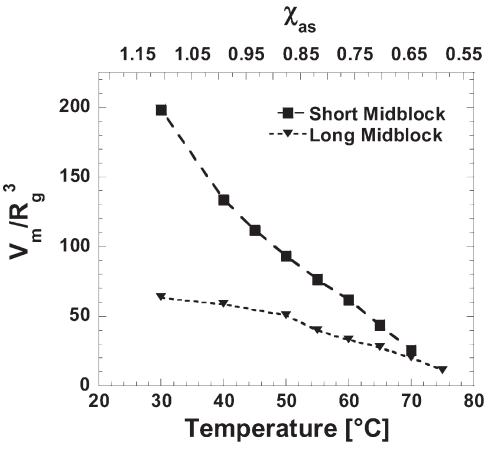

Figure 2. Equilibrium micelle volume as a function of temperature for the short-midblock and long-midblock systems at $\Phi_p = 0.15$.

Gel Structure. For each temperature, SCFT calculations were iterated for a range of micelle sizes. Figure 1 is a representative plot of the free energy as a function of R. Arrows indicate the location of free energy minima, which define the equilibrium micelle sizes, R_{eq}, and the corresponding equilibrium free energies. The equilibrium free energy increases toward the value of zero for a homogeneous solution as the temperature increases, while R_{eq} decreases. The temperature dependence of the micelle size for a representative case is shown in Figure 2, where we plot the temperature dependence of the volume per micelle, V_m, defined as follows:

$$V_m = \frac{4}{3}\pi {R_{eq}}^3 \tag{10}$$

As temperature increases, the equilibrium volume per micelle decreases, as does the aggregation number, M, the number of A end blocks in each micelle core. The aggregation number is linearly related to V_m by the following expression:

$$M = \frac{2\rho\Phi_p N_{av}}{M_n} V_m \tag{11}$$

where ρ is the density of the triblock copolymer, Φ_p is the overall volume fraction of polymer in solution, M_n is the triblock molecular weight, and N_{av} is Avogadro's number.

It is clear from Figure 2 that the aggregation number decreases more rapidly with temperature in the short-midblock polymer system than long-midblock polymer system. To understand why this occurs, it is helpful to compare the volume fraction profiles of the two chemical components, A and B, of both systems. Figure 3 shows the volume fraction profiles for long and short-midblock polymer micelles for $\Phi_p = 0.15$ at 50 °C. At 50 °C, we see that each micelle consists of a core of end block surrounded by a corona of midblock.

The difference in midblock content between the two polymers studied is apparent in the volume fraction profiles for the B midblocks. For the short-midblock $\phi_B(r)$ in the coronal region drops off to almost zero near R_{eq}. In contrast, the long-midblock system shows only a slight decrease in $\phi_B(r)$ in the coronal region. As a result, the bridging fraction is much lower in the short-midblock copolymer gel than in

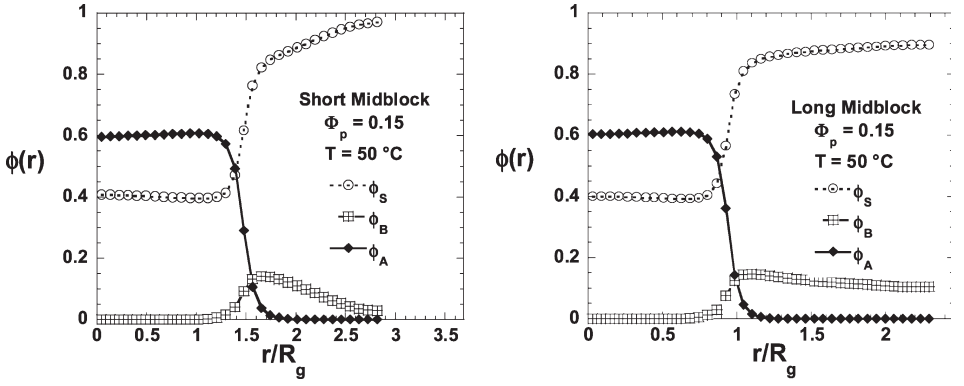

Figure 3. Representative volume fraction profiles for each component in short-midblock and long-midblock gels.

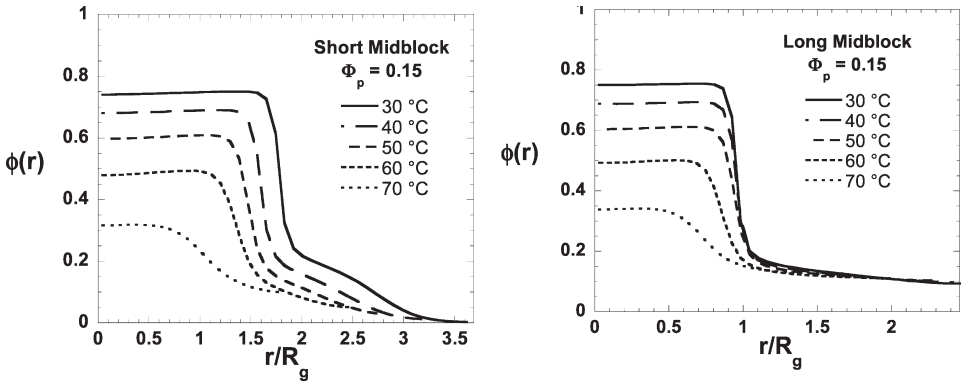

Figure 4. Temperature dependence of the overall polymer volume fraction profiles for the short-midblock and long-midblock copolymers.

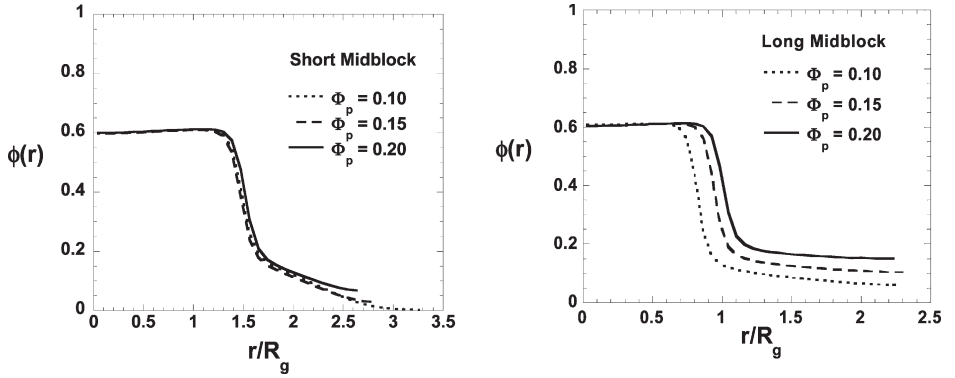

Figure 5. Concentration dependence of the overall polymer volume fraction profiles for the short-midblock and long-midblock copolymers at 50 °C.

the long-midblock copolymer gel, a fact that is quantified in more detail below.

The temperature dependencies of the overall polymer volume fraction for gels with $\Phi_p = 0.15$ are compared in Figure 4. Several trends are observed. First, the aggregation number and overall volume fraction of A in the micelle core decrease with increasing temperature. Also, at any given temperature the short-midblock and long-midblock gels both have similar polymer fractions in the micelle core. More substantial differences are observed in the coronal regions of the gel structure. Because the midblocks are less strongly stretched in the long-midblock copolymer, the midblocks in this system can more easily fill the space between micelle cores.

This difference in the behavior of the two different copolymers leads to a variety of important consequences with regard to the concentration dependence of the aggregation number and bridging fraction. These concentration effects are demonstrated in Figure 5 for the short-midblock and long-midblock copolymers. For both polymers the variation in the total copolymer volume fraction has very little impact on the solvent content of the micelle cores. Apart from this similarity, we observe very different behavior for the long-midblock and short-midblock copolymers. For the long-midblock copolymer the average micelle size, given by R_{eq} is roughly independent of polymer concentration. For this polymer the size of the micelle is determined largely by the chain stretching of the midblocks, and the aggregation number is proportional to the overall polymer concentration. For the short-midblock copolymer, the opposite situation is observed, with the aggregation number remaining independent of the overall polymer concentration. Because the equilibrium polymer concentration at the midpoint between adjacent micelles is quite low in this case, the

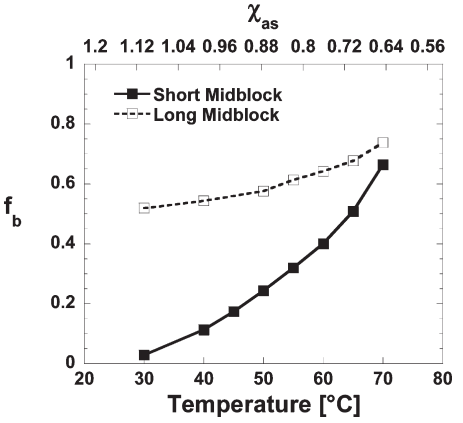

Figure 6. Temperature dependence of the bridging fraction for gels with $\Phi_p = 0.15$.

bridging fraction is also low, and the aggregation number is close to the value obtained in the low-concentration limit where all of the midblocks are in looping configurations.

Bridging Fraction. The equilibrium bridging fraction is plotted as a function of temperature for both polymers in Figure 6 for gels with $\Phi_p = 0.15$. Because of the greater importance of chain stretching for the short-midblock system, the bridging fraction for this system has a higher temperature dependence than it does for the long-midblock system. At 30 °C less than 5% of the short-midblock chains form bridges, while more than 50% of the chains form bridges in the long-midblock gel. When comparing to experimental data, it is important to remember that true equilibrium will not be obtained when the relaxation time associated with end block exchange between micelle cores

is longer than the experimental time scale. In these cases the bridging fraction and aggregation number may become frozen at values corresponding to the equilibrium values at higher temperatures. The ability to freeze the gel structure into nonequilibrium states is an important factor in the design of gels with the desired properties.

Osmotic Properties. The swelling properties of the polymer gels can be obtained by consideration of the solvent chemical potential. The link to our calculations is through the osmotic pressure Π, which is directly related to the solvent chemical potential:

$$\Pi = \frac{-\Delta\mu_s}{V_0} \tag{12}$$

Here $\Delta\mu_s$ is the chemical potential of the solution relative to pure solvent and V_0 is the solvent molecular volume. In order to remove detailed effects associated with the model used to describe the polymer/solvent interactions, it is useful to introduce the concept of an equivalent polymer volume fraction when describing osmotic pressure. We define this equivalent volume fraction as the volume fraction of infinite molecular weight polymer that gives the same osmotic pressure as the value obtained from the SCFT calculations. Two different equivalent volume fractions, ϕ_a^μ and ϕ_b^μ, are defined by the following Flory−Huggins expressions for the solvent chemical potentials:

$$\mu_s = \begin{cases} \ln(1-\phi_a^\mu)+\phi_a^\mu+\chi_{as}(\phi_a^\mu)^2 \\ \text{or} \\ \ln(1-\phi_b^\mu)+\phi_b^\mu+\chi_{bs}(\phi_b^\mu)^2 \end{cases} \tag{13}$$

Furthermore, the equivalent volume fractions where $\mu_s = 0$, that is, when the chemical potential of the solution is at equilibrium with pure solvent, are defined as ϕ_a^0 and ϕ_b^0. These quantities only exist when the corresponding polymer/solvent interaction parameter is greater than 0.5 and in our case only applies to the A component. In addition to the conceptual utility of the equivalent volume fractions, they are also of practical significance when interpreting experimental osmotic pressure data for block copolymer solutions. Methods such as vapor pressure osmometry require that calibration solutions be used. By presenting our results in terms of these equivalent volume fractions, we facilitate direct comparisons to experimental results that use homopolymer solutions as calibration standards.

Figure 7 shows the values of ϕ_a^μ and ϕ_b^μ for gels made from both copolymers, with $\Phi_p = 0.15$. For all temperatures except for those very close to the ordering transition, ϕ_a^μ is very close to ϕ_a^0, indicating that the volume fraction of solvent in the core is nearly identical to the solvent fraction in a high molecular weight polymer that is equilibrated with pure solvent. The result appears to be very general and suggests a useful procedure for estimating the solvent fraction in micellar aggregates. This procedure was previously assumed to be valid[8] but has not been rigorously tested until now.

Values for ϕ_b^μ are also instructive and relate more directly to the swelling behavior of the gels. A value of 0 for ϕ_b^μ is obtained when the gel is in equilibrium with pure solvent, so that $\Pi = 0$. Negative values for Π are not thermodynamically stable, since the gel will undergo syneresis, ejecting solvent until Π and ϕ_b^μ are both zero. This situation is not observed for any of the data plotted in Figure 7. Again, the situation changes if the gels are not completely at equilibrium. For example, "constrained equilibrium" calculations, where the aggregation number of the gels is fixed to correspond to the equilibrium values at 55 °C, give values for ϕ_b^μ that reach zero at lower temperatures. The situation is actually quite difficult to handle within the context of SCFT theory. It is simple to keep the aggregation number constant by keeping R fixed at the value of interest, but it is much more difficult to add a constraint that the bridging fraction also remains constant, as it must in a true experimental system where end block exchange between aggregates is kinetically prohibited.

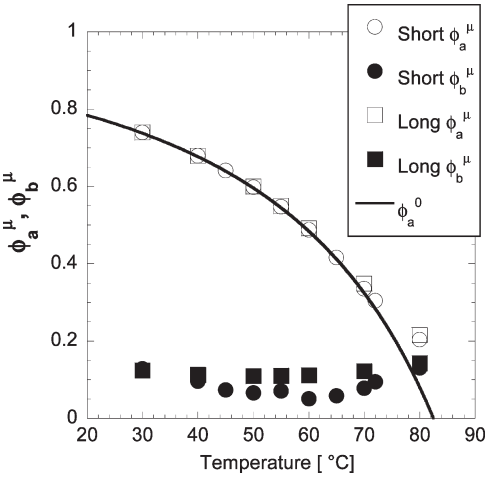

Figure 7. Temperature dependence of the equivalent polymer volume fractions for polymer gels with $\Phi_p = 0.15$. Data for short-midblock and long-midblock copolymers are included, as indicated in the legend.

X-ray Scattering Intensity. SCFT calculations can also be used to simulate small-angle X-ray scattering results. Small-angle X-ray scattering is a useful tool for studying the structure of polymer melts and gels. The intensity of scattered X-rays in reciprocal space, $I(q)$, is the square of the scattering amplitude, $A(q)$, which can be expressed as the Fourier transform of the scattering length density, $\rho(r)$, over the illuminated volume:

$$I(q) = |A(q)|^2 \propto \left|\int_V \rho(r) e^{-iqr}\right|^2 \tag{14}$$

where q is the scattering vector. Assuming incompressibility and no volume change upon mixing, it is a simple process to convert volume fraction profiles of the various chemical components to scattering length densities. For X-rays, which scatter primarily from electrons, the relevant quantity is the electron density in the sample:

$$\rho(r) = r_e \sum_{m=a,b,s} n_m(r) \tag{15}$$

where r_e is the electron scattering length and $n_m(r)$ is the local electron density of component n. The specific expression for average electron density is related to the volume fraction of a component by

$$n_m(r) = \phi_m(r)\frac{N_{av}\rho_m e_m}{M_w} \tag{16}$$

where N_{av} is Avogadro's number, ρ_m is the component density, e_m is the number of electrons per repeat unit, and M_w is the repeat unit molecular weight. For the acrylic model system that we are fitting, the end-block-rich regions dominate the scattering length density profiles as PMMA is significantly more electron dense than the solvent. In this case the electron scattering length density profiles are similar

in shape to the volume fraction profiles for the core forming shown in Figure 4.

In situations where the characteristic size of the scattering centers is substantially smaller than their average separation, it is convenient to express the scattered intensity as the product of a form factor, $f(q)$, that is determined by the shape of the scattering center and a structure factor, $S(q)$, that describes the interference of radiation interacting with these different centers.[36] In this case eq 14 is written as

$$I(q) \propto N|f(q)|^2 S(q) \tag{17}$$

where N is the number of scattering centers, each with a form factor $f(q)$. The previous use of the unit cell approximation in these SCFT calculations provides a good estimate of the average nearest-neighbor distance, but further information as to the aggregate organization is lost. Therefore, calculations of the expected SAXS results are limited to the calculation of the form factor, which for a single spherical symmetric object is given by the following expression:

$$f(q) = \int_0^\infty \rho(r) \frac{4\pi r^2 \sin(qr)}{qr} \, dr \tag{18}$$

In the SCF calculations the integral extends from $r = 0$ to $r = R$, the location of the reflecting boundary condition. Because scattering methods are only sensitive to differences in electron density, we subtract the scattering length density at $r = R$ to obtain the following for $f_{scf}(q)$, the form factor calculated from SCF theory:

$$f_{scf}(q) = \int_0^R (\rho(r) - \rho(R)) \left(\frac{4\pi r^2 \sin(qr)}{qr} \right) dr \tag{19}$$

Because the scattering is dominated by the micelle cores which have a nearly uniform composition, it is possible to approximate the form factor by approximating the scattering centers as spheres of radius r_0 and a constant scattering length density:

$$\rho(r) - \rho(R) = \begin{cases} \rho_0 & r \le r_0 \\ 0 & r > r_0 \end{cases} \tag{20}$$

This step function form for the scattering length density profile results in the following expression for the form factor, which we refer to as the hard-sphere form factor, f_{hs}:[36]

$$f_{hs}(q) = \rho_0 V_c \left\{ \frac{3}{(qr_0)^3} [\sin(qr_0) - qr_0 \cos(qr_0)] \right\} \tag{21}$$

where V_c is the volume of a micelle core, i.e., $V_c = 4\pi r_0^3/3$.

At this point we are in a position to obtain values of r_0 and ρ_0 from the SCF theory and to compare this value of f_{hs} to the form factor obtained using the detailed electron density profile from the SCFT calculations. Values of r_0, taken as the point of maximum slope in a plot of $\rho(r)$, are shown in Figure 8 for both long- and short-midblock polymers as a function of temperature. Corresponding values of ρ_0, defined as the average scattering length density between $r = 0$ and $r = 0.9r_0$, are shown in Figure 9. Because we are primarily interested in the temperature dependence of the scattering intensity, values of ρ_0 are normalized by the values at 30 °C. Values of χ_{as}, the interaction parameter between the solvent and the end blocks (obtained from eq 8), are included in Figures 8 and 9 as well.

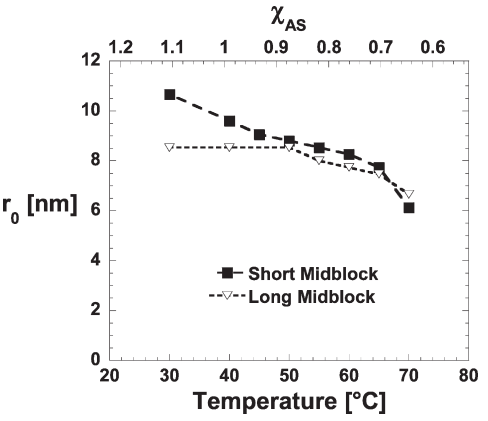

Figure 8. Temperature dependence of the radius of the micellar cores.

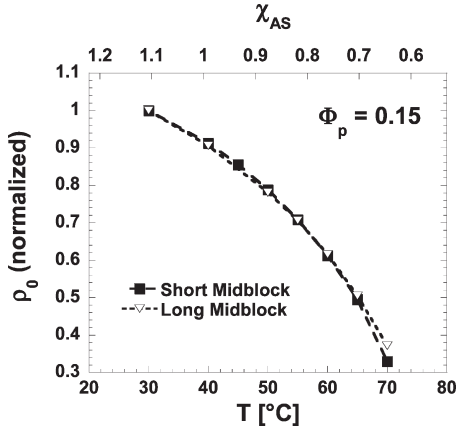

Figure 9. Temperature dependence of the scattering length density contrast, normalized to the contrast obtained at 30 °C.

Using either the numerical integration or step function approximations to compute the scattering intensity gives similar results as illustrated in Figure 10, which shows calculated values of the form factor at 30 °C for both short- and long-midblock copolymers. Values of f_{scf} were obtained from eq 19, using the full radial dependence of the electron scattering length as calculated from the SCF theory. Values of f_{hs} correspond to eq 21, using the values for the scattering length density contrast plotted in Figure 9. This information can be used to estimate the temperature dependence of the scattering intensity. The temperature dependence of the scattering amplitude can be estimated by taking the $q = 0$ limit, which is determined by the temperature dependence of the form factor. The number of aggregates, N, is inversely proportional to the aggregation number, which is in turn proportional to the micelle volume, V_m. In addition $V_c \propto r_0^3$, so using the hard-sphere version of the form factor, eq 17 reduces to the following for the $I_{hs}(0)$, the scattering intensity for the hard-sphere model at $q = 0$:

$$I_{hs}(0) \propto N\rho_0^2 V_c^2 \propto \rho_0^2 r_0^6 / V_m \tag{22}$$

Each of the quantities in eq 22 has been determined from the SCF theory, with ρ_0 plotted in Figure 9, r_0 in Figure 8, and V_m in Figure 2. The temperature dependence of $I_{hs}(0)$ obtained from these data and from eq 22 is plotted in Figure 11a, normalized to the value at 30 °C. Values for $I_{scf}(0)$ are shown in Figure 11b. In this case the form factor obtained from the full SCF calculation is used,

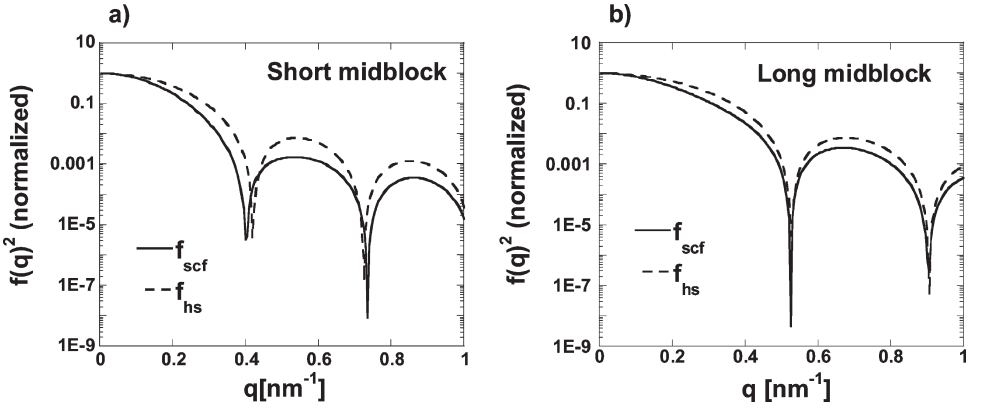

Figure 10. Form factors calculated from the hard-sphere model (eq 21) and from the full SCF calculation (eq 19) for gels with $\Phi_p = 0.15$ and $T = 30$ °C.

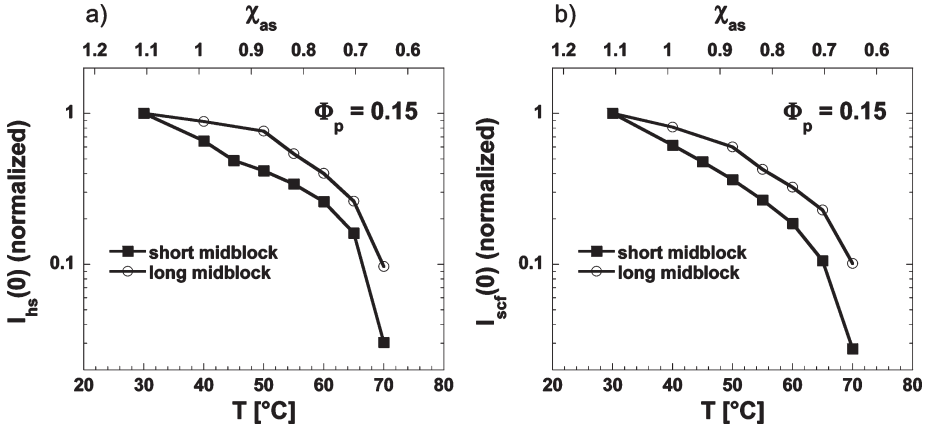

Figure 11. Temperature dependence of the scattered intensity at zero angle from the hard-sphere approximation (eq 22, part a) and from the full SCF electron scattering length distribution of (eq 23, part b).

so that the low-angle scattering is given by the following expression:

$$I_{\mathrm{scf}}(0) \propto {f_{\mathrm{scf}}}^2(0)/V_m \tag{23}$$

Several important conclusions can be drawn from intensity data shown in Figure 11. The first is that the hard-sphere approximation works very well and captures the essence of the temperature transition. More importantly, the results are in good agreement with experimentally determined temperature dependence of the scattering amplitude in these types of polymers.[4] These results are also consistent with the assumption made in this previous experimental work that the observed intensity increase is not due to an increase in fraction of block copolymers that were in micellar form. This observed temperature dependence can be attributed to the temperature dependence of micellar structure, and the effect this structure has on the scattering intensity from an isolated micelle. In the experimental system the scattered intensity is roughly constant at temperatures below about 55 °C. This result can be understood by the fact that at these low temperatures the relaxation time of the micellar cores is high enough so that they can no longer equilibrate. The total number of micelles, and the aggregation number of each micelle, remain constant as the temperature is reduced further. The micelle cores get denser, but the quantity $\rho_0 V_c$ remains roughly fixed. This situation can be accounted for in the SCF calculations by running a series of calculations at a fixed value of R. Calculations of this sort confirm our expectation under this "constrained equilibrium" situation: the form factor of the micelles becomes temperature independent.

Conclusions

Self-consistent field theory can be a very useful tool in modeling complex polymeric systems. Appropriate choice of input parameters allows comparison to experimental results and provides structural information that is very difficult to obtain by other theoretical means. We have utilized a unit cell approximation that is able to provide information about individual micelles but which does not provide information about preferred 3-dimensional packing of the micellar aggregates. In situations where the micelles are not organized on a crystalline lattice, as is often the case experimentally, this unit cell approximation is all that is required in order to provide information about the preferred micellar geometry (spheres, cylinders, or lamellar), the aggregation number, bridging fraction, solvent osmotic pressure, and form factor for a scattering experiment.

The specific calculations performed here are motivated by experimental data that exist for two closely related triblock copolymers. When dissolved in appropriate solvents, these block copolymers form thermoreversible gels. The data have been presented in terms of temperatures that are experimentally relevant for this system and also in terms of thermodynamic chi parameters describing the interactions between the solvent and the end blocks. From these results we were able to arrive at a number of more general conclusions, including the following:

- The solvent in the micelle cores is distributed quite homogeneously at a volume fraction nearly identical

to the corresponding value for a pure, high molecular weight homopolymer in pure solvent.

- As the solvent quality for the end blocks decreases and solvent is expelled from the micelle cores, the equilibrium aggregation number increases and the equilibrium bridging fraction decreases. The increased aggregation number is primarily responsible for the observed increase in the scattering intensity from a small-angle X-ray scattering experiment.
- As the polymer concentration is decreased, the bridging fraction also decreases. This decrease occurs at higher concentrations for the short-midblock polymers, where the midblocks must be highly stretched in order to adopt bridging conformations. As the bridging fraction becomes very small, the aggregation numbers approach value corresponding to the dilute limit that is nearly independent of the concentration.
- The osmotic properties of the gel were expressed in terms of an equivalent solution of high molecular weight midblock homopolymer that has the same solvent chemical potential. The polymer concentration of this equivalent solution initially decreases as the solvent quality for the end blocks is decreased but increases again as the bridging fraction begins to decrease substantially.

Acknowledgment. This work was supported through the NSF MRSEC program (DMR-0520513) and through the NSF Polymers Program (DMR-0525645). We are grateful to Dr. M. E. Seitz for helpful comments and for providing a critical reading of the manuscript.

References and Notes

(1) Ruzette, A. V.; Leibler, L. *Nat. Mater.* **2005**, *4*, 19.
(2) Segalman, R. A. *Mater. Sci. Eng., R* **2005**, *48*, 191–226.
(3) Baroli, B. *J. Pharm. Sci.* **2007**, *96*, 2197–2223.
(4) Seitz, M. E.; Burghardt, W. R.; Faber, K. T.; Shull, K. R. *Macromolecules* **2007**, *40*, 1218–1226.
(5) Semenov, A. N.; Joanny, J.; Khokhlov, A. R. *Macromolecules* **1995**, *28*, 1066–1075.
(6) Seitz, M. E.; Martina, D.; Baumberger, T.; Krishnan, V. R.; Hui, C.; Shull, K. R. *Soft Matter* **2009**, *5*, 447–456.
(7) Flanigan, C. M.; Crosby, A. J.; Shull, K. R. *Macromolecules* **1999**, *32*, 7251–7262.
(8) Drzal, P. L.; Shull, K. R. *Macromolecules* **2003**, *36*, 2000–2008.
(9) Edwards, S. *Proc. Phys. Soc. London* **1965**, *85*, 613.
(10) Orland, H.; Schick, M. *Macromolecules* **1996**, *29*, 713–717.
(11) Shull, K. *Macromolecules* **1996**, *29*, 2659–2666.
(12) Matsen, M. W. *Macromolecules* **2003**, *36*, 9647–9657.
(13) Matsen, M. W.; Schick, M. *Macromolecules* **1994**, *27*, 4014–4015.
(14) Matsen, M. W.; Thompson, R. B. *J. Chem. Phys.* **1999**, *111*, 7139–7146.
(15) Matsen, M. W. *J. Chem. Phys.* **2000**, *113*, 5539–5544.
(16) Mai, S. M.; Fairclough, J. P. A.; Hamley, I. W.; Matsen, M. W.; Denny, R. C.; Liao, B. X.; Booth, C.; Ryan, A. J. *Macromolecules* **1996**, *29*, 6212–6221.
(17) Matsen, M. W.; Bates, F. S. *Macromolecules* **1996**, *29*, 7641–7644.
(18) Linse, P. *J. Phys. Chem.* **1993**, *97*, 13896–13902.
(19) Noolandi, J.; Shi, A. C.; Linse, P. *Macromolecules* **1996**, *29*, 5907–5919.
(20) Lefebvre, M. D.; Shull, K. R. *Macromolecules* **2006**, *39*, 3450–3457.
(21) Wang, R.; Tang, P.; Qiu, F.; Yang, Y. *J. Phys. Chem. B* **2005**, *109*, 17120–17127.
(22) He, X.; Liang, H.; Huang, L.; Pan, C. *J. Phys. Chem. B* **2004**, *108*, 1731–1735.
(23) Drolet, F.; Fredrickson, G. H. *Phys. Rev. Lett.* **1999**, *83*, 4317–4320.
(24) Drolet, F.; Fredrickson, G. H. *Macromolecules* **2001**, *34*, 5317–5324.
(25) Bohbot-Raviv, Y.; Wang, Z. G. *Phys. Rev. Lett.* **2000**, *85*, 3428–3431.
(26) Nunalee, M. L.; Guo, H.; Olvera de la Cruz, M.; Shull, K. R. *Macromolecules* **2007**, *40*, 4721–4723.
(27) Sides, S. W.; Fredrickson, G. H. *Polymer* **2003**, *44*, 5859–5866.
(28) Wu, Y. Y.; Cheng, G. S.; Katsov, K.; Sides, S. W.; Wang, J. F.; Tang, J.; Fredrickson, G. H.; Moskovits, M.; Stucky, G. D. *Nat. Mater.* **2004**, *3*, 816–822.
(29) Gompper, G.; Schick, M. *Soft Matter*; Wiley-VCH: Weinheim, 2006.
(30) Helfand, E.; Wasserman, Z. *Macromolecules* **1976**, *9*, 879.
(31) Vavasour, J.; Whitmore, M. *Macromolecules* **1992**, *25*, 5477.
(32) Shi, A. C.; Noolandi, J. *Macromolecules* **1994**, *27*, 2936–2944.
(33) Shull, K. *Macromolecules* **2002**, *35*, 8631–8639.
(34) Lefebvre, M. D.; Olvera de la Cruz, M.; Shull, K. R. *Macromolecules* **2004**, *37*, 1118–1123.
(35) Jenckel, V.; Gorke, K. *Z. Naturforsch.* **1950**, *5A*, 556.
(36) Svensson, B.; Olsson, U.; Alexandridis, P.; Mortensen, K. *Macromolecules* **1999**, *32*, 6725–6733.